Universitat Autònoma
de Barcelona

BACHELOR'S THESIS

Degree in Physics

Nanoscale Heat Transport Study by Monte Carlo Simulations

Àlex Giménez Romero
1420683

Course
2018/19

Supervisor
Xavier Àlvarez Calafell

Call
July

To all my family, friends and those who I've ever met,
without whom I wouldn't be who I am.

Acknowledgements

This work would not have been possible without the supervision of Dr. Xavier Àlvarez Calafell, whom I would like to thank for his guidance, advisement and patience. I also would like to thank Dr. Jordi Faraudo, Dr. Juan Camacho and Dr. David Malaspina with whom I have had the pleasure to work recently and have left a professional mark on me, which I hope I can transmit in this thesis. I also would like to thank them for all the advises given to me and their free teaching, which I strongly value.

I am grateful to all of those with whom I have had the pleasure to share this degree in Physics during these four years, which despite being hard years in different senses, will be always in my mind. I also would be pleased to acknowledge my childhood friends, who have really motivated me in my worst moments and brought me always a smile.

Finally, a special thank to my family for all the love and support given to me.

Abstract

Nowadays electronic nanodevices have experimented a considerable increase in popularity and utility due its applications in energy transport, storage and conversion as well as future applications in electronics. As in every electronic device, the influence of temperature must be taken into account, as it is directly related with some electric or thermoelectric properties of the material. This characterisation can be done by studying the properties of heat transport in the material used to build the object in the appropriate spatial scale. Then, it was observed that the classical Fourier's diffusive equation gives erroneous results when applied to this kind of systems and therefore a need for the study of heat transport at nanometric scales gave rise.

This work studies heat transport in germanium nanostructures through computer simulations using a simplified Monte Carlo method, known as Gray Model. To fully understand the method, the concept of phonon as a quasiparticle needs to be introduced and explained properly along with the Boltzmann Transport Equation (BTE), which plays an important role in the implementation of the Monte Carlo method . For this reason a theory section is included, where the classical and quantum treatment of the heat transport is shown together with the BTE. Then the Gray Model is acutely explained before the presentation of the results, ending all up with the corresponding conclusions.

Contents

1 Introduction

Heat conduction has been modeled for almost two centuries by the well known Fourier's Law. Joseph Fourier stated that "the quantity of heat which flows uniformly, during unit of time, across unit of surface taken on any section whatever parallel to the sides, all other things being equal, is directly proportional to the difference of the extreme temperatures, and inversely proportional to the distance which separates these sides" [1]. The differential form of Fourier's law of thermal conduction shows that the local heat flux density[1], $\boldsymbol{q}$, is equal to the product of thermal conductivity, k, and the negative local temperature gradient $\boldsymbol{\nabla} T$, so it can be written as follows

$$\boldsymbol{q} = -k\boldsymbol{\nabla} T \tag{1}$$

Eq. 1 joined with the continuity equation for thermal flux gives the well known diffusive heat conduction equation

$$\rho C_p \frac{\partial T}{\partial t} + \boldsymbol{\nabla} \cdot \boldsymbol{q} = H \tag{2}$$

where ρ is the material density, C_p is the specific heat capacity and H is the sum of all the heat sources in the system . If the sum of the heat sources is equal to zero we reach the diffusion equation applying the divergence to the gradient of Eq. (1)

$$\rho C_p \frac{\partial T}{\partial t} - k\nabla^2 T = 0 \Longrightarrow \frac{\partial T}{\partial t} - \frac{k}{\rho C_p}\nabla^2 T = 0 \Longrightarrow \frac{\partial T}{\partial t} = D\nabla^2 T$$

While Fourier's law is valid at the macroscale, it has been experimentally proved that in some nanostructured materials, such as nanowires, thin films or nanoporous materials, the description of thermal transport as diffusive heat conduction breaks down. [2]

Nowadays we know that heat conduction in a crystalline material takes place through lattice vibrations. This lattice is a three dimensional structure formed by the atoms of the solid held together by atomic bonds. Under the influence of temperature, the atoms oscillate about their mean equilibrium positions, so that the amplitudes of this oscillations increase with the increase in temperature of the solid. When an atom is displaced from its equilibrium position, vibrational waves are created, carrying energy while propagating through the crystal. The propagation of this waves with the energy they carry, and the interaction between each other is what gives rise to heat transfer. It can be shown using second quantization techniques that this waves have particle properties, similarly to photons, so they are understood as particle-like waves called phonons. Every phonon is characterised by its frequency ω , wave vector k and polarization p. The quantum of energy contained by a phonon is given by $\hbar\omega$ where $\hbar$ is the reduced Planck's constant, to say Planck's constant divided by 2π. So, at the end, heat transfer in a crystalline material can be visualised as phonon interactions.

The underlying assumption in Fourier's law is that heat is transferred from one region to another subject to sufficient phonon scattering events, as it is a diffusion equation. If the material size is much larger than the phonons *mean free path*[2] many scattering events will take place so that local thermodynamic equilibrium is restored in the material. Due to this mechanism we have a diffusive thermal transport by which a temperature gradient is established within the medium, corresponding to what is obtained solving the Fourier's heat equation. However, when the phonon's mean free path is larger than the material's size there is no significant scattering events, so the thermal transport is in its ballistic regime, where the thermal conductivity of the material is governed by boundary and impurity scattering processes. In such cases, Fourier's Law is no longer valid to describe the thermal transport process, since it is not a diffusive process.

To study the ballistic regime above mentioned a new approach has been taken in the form of the Boltzmann Transport Equation (BTE). Assuming that the particle-like behaviour of phonons is much more significant than its wave-like behaviour makes possible for the BTE to solve ballistic

[1] Amount of energy that flows through a unit area per unit time
[2] Distance travelled by the phonon before going into a scattering event.

phonon transport at nanoscale when the size of the material is smaller than the mean free path of the phonons but larger than its wave length [1]. In addition, it is assumed that phonons follow Bose-Einstein statistics and interact with each other via scattering processes. [3]

The BTE applyed to phonons can be expressed as follows

$$\frac{\mathrm{d}f}{\mathrm{d}t} + v_g \boldsymbol{\nabla} f = \left(\frac{\mathrm{d}f}{\mathrm{d}t}\right)_{scattering} \tag{3}$$

where f is the distribution function of an ensemble of phonons, to say bose-einstein distribution function and v_g is the group velocity. Clearly, the left hand side (LHS) of the BTE represents the change on the distribution function due to the phonon drift, while the right hand side (RHS) shows the change in the distribution function due the scattering events. Physically, drift causes energy distribution function to deviate from equilibrium whereas the scattering process tends to restore it.

To solve BTE analytically several assumptions have to be made in order to bring the equation to a simplified solvable form, which can alter the real dynamics of phonon transport. On the other hand, statistical computational methods such as the Monte Carlo (MC) method can be used to solve the whole BTE without any simplification. The aim of this work is to perform a MC simulation to solve numerically the BTE and study the thermal transport in different regimes and situations.

[1] We need the characteristic size of the material to be greater than the phonon wave length to consider phonons as particles.

2 Theory

2.1 Phonons as crystal lattice vibrations

One can consider a crystal lattice as a three dimensional structure of masses held by springs, which correspond to the atoms and chemical bonds that form the solid. Then, thermal energy transport can be understood in terms of atom vibrations caused by oscillations about their mean equilibrium positions, so that their amplitudes increase with the increase in temperature of the solid. As the materials subject to our study is germanium, with two atoms in a primitive cell, let us consider a unit cell formed by two atoms with masses m_1 and m_2 held together by a spring of natural length l and elastic constant k_e. Assuming linearity, that is to say $F_i = -k_e r_i$ and nearest neighbours interaction we are able to find the normal modes of vibrations. As the three directions of vibration are independent of each other, we will do the analysis in one dimension and will be extended then to a three dimensional setup of masses and springs. [3]

Let x_1^n and x_2^n be the displacements of masses m_1 and m_2 in the n^{th} unit cell from their equilibrium positions, then the equations of motion for masses m_1 and m_2 are given by

$$\begin{aligned} m_1 \tfrac{\mathrm{d}^2}{\mathrm{d}t^2} x_1^{(n)} &= k_e \left(x_2^{(n)} + x_2^{(n-1)} - 2x_1^{(n)} \right) \\ m_2 \tfrac{\mathrm{d}^2}{\mathrm{d}t^2} x_2^{(n)} &= k_e \left(x_1^{(n)} + x_1^{(n-1)} - 2x_2^{(n)} \right) \end{aligned} \tag{4}$$

The solution for this differential equations have the form of plane waves, so they can be written as follows [4]

$$\begin{aligned} x_1^n &= A e^{i(nka - \omega t)} \\ x_2^n &= B e^{i(nka - \omega t)} \end{aligned} \tag{5}$$

Where A and B are the amplitudes of the waves, ω it's freqüency and k is the wave vector given by $k = 2\pi/\lambda$.

Now, substituting the equations in Eq. (5) into the equations of the motion, one obtains a solvable system of homogeneous linear equations, which can be expressed in matrix form

$$\begin{pmatrix} 2k_e - m_1\omega^2 & -k_e(1 + e^{-ika}) \\ -k_e(1 + e^{ika}) & 2k_e - m_2\omega^2 \end{pmatrix} \begin{pmatrix} A \\ B \end{pmatrix} = \begin{pmatrix} 0 \\ 0 \end{pmatrix} \tag{6}$$

In order to get the non-trivial solution the determinant of the coefficient matrix must vanish, so we can reduce the system of equations to a single one

$$m_1 m_2 \omega^4 - 2k_e \left(m_1 + m_2\right) \omega^2 + 2k_e^2 \left(1 - \cos ka\right) = 0 \tag{7}$$

Solving for ω^2 we obtain

$$\omega^2 = k_e \left(\frac{1}{m_1} + \frac{1}{m_2} \right) \left[1 \pm \sqrt{1 - \frac{4m_1 m_2}{\left(m_1 + m_2\right)^2} \sin^2 \left(\frac{ka}{2} \right)} \right] \tag{8}$$

The above relation between ω and k is called the dispersion relation $\omega(k)$. The two possible solutions for the frequency given by the dispersion relation are called the optical and acoustical branches. In the optical mode the atoms vibrate against each other while the centre of mass remains fixed. If the two atoms carry opposite electric charge this kind of movement can be excited by the electric field of a light wave, so for this reason is called optical mode. In the acoustic mode the atoms and its centre of mass move together, as in long wavelength acoustical vibrations [4]. A graphical representation of this two vibrational modes is show in in Fig. 1

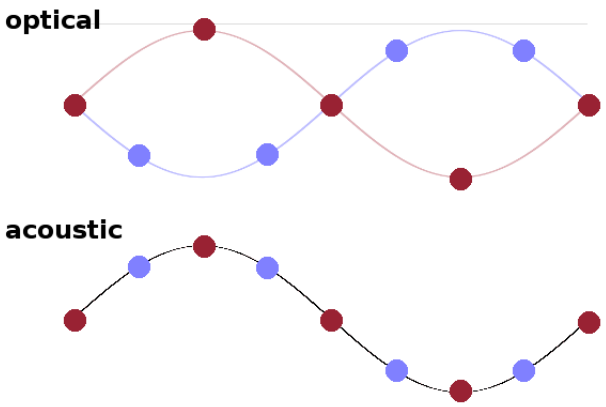

Figure 1: Acoustic and optic modes

The plot for $\omega(k)$ of this two vibrational modes is shown in figure Fig. 2.Clearly because of the dependence of ω to the squared sinus of k, the frequency is periodic along the different possible wave vectors with a period of $2\pi/a$. These periodic zones are called Brillouin zones, and when $k \in [-\pi/a, \pi/a]$ is called the first Brillouin zone. Due the periodicity of the dispersion relation, only the k values within the first Brillouin zone are physically relevant, as the ones out of this zone merely reproduce the same values of ω as described in the first Brillouin zone.

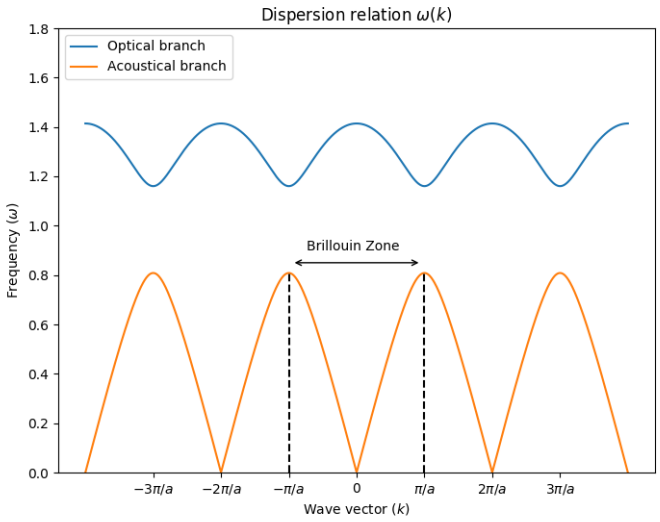

Figure 2: Dispersion relation plot for $m_1 = 2m_2$

Then, we can examine the dispersion relation in the Brillouin zone limiting cases: $ka \ll 1$ and $ka = \pm\pi/a$.

- For $ka \ll 1$ we can make a Taylor expansion for the squared sinus and the square root, where $sin^2(x) \simeq x^2$ and $\sqrt{1-x} \simeq 1 - \frac{1}{2}x$. Then we find two possible frequencies

$$w_1{}^2 = 2k_e \frac{1}{m_1 + m_2} \quad \text{(Optical branch)} \tag{9}$$

$$w_2{}^2 = \frac{1}{2} k_e \frac{k^2 a^2}{m_1 + m_2} \quad \text{(Acoustical branch)} \tag{10}$$

- For $k = \pm\pi/a$ the two possible frequencies are

$$\omega_1{}^2 = 2k_e/m_2 \quad \text{(Optical branch)} \tag{11}$$

$$\omega_2{}^2 = 2k_e/m_1 \quad \text{(Acoustical branch)} \tag{12}$$

  Where $m_1 > m_2$ for consistency with Fig. 2

If we generalise this development to a three dimensional system of masses and springs, with three degrees of freedom, we will end up with six equations of motion which conform a 6x6 dynamical matrix. Hence, a 3-D unit cell with two atoms per cell has six phonon vibrational modes: three acoustic and three optical. Moreover, each one has two transverse branches and a longitudinal branch [3]. Even more generally, if we had p atoms per unit cell the dispersion relation would have $3p$ vibrational modes: 3 acoustic and $3p-3$ optical modes [4].

2.2 Phonons as quasiparticles: the quantization of elastic waves

In order to show that phonons can be understood as quasiparticle bosons we just need to take into account the quantum theory. As before, we consider a set of N particles of mass m connected by springs of elastic constant k_e and situated at a distance a from each other in their equilibrium positions. For simplicity, we will just consider a single atom for unit cell. The displacement of the particle s is given by q_s and its momentum by p_s. Then, the Hamiltonian of the system is the sum of the kinetic and potential energy of each particle

$$H = \sum_{s=1}^{N} \left\{ \frac{{p_s}^2}{2m} + \frac{1}{2} k_e \left(q_{s+1} - q_s\right)^2 \right\} \tag{13}$$

We already know from basic quantum theory that the Hamiltonian of an harmonic oscillator is given by

$$H = \frac{p^2}{2m} + \frac{1}{2} m\omega^2 \tag{14}$$

and that its eigenvalues, that is to say the energy of each eigenstate (or eigenvector) of the Hamiltonian, are

$$\varepsilon_n = \hbar\omega \left(n + \frac{1}{2}\right) \quad \text{with} \quad n = 0, 1, 2, 3... \tag{15}$$

Making a Fourier transformation from the coordinates q_s and p_s to the new coordinates Q_k and P_k, known as *phonon coordinates*. The change of coordinates is given by

$$\begin{aligned} q_s &= \frac{1}{\sqrt{N}} \sum_k Q_k e^{iksa} \\ p_s &= \frac{1}{\sqrt{N}} \sum_k P_k e^{-iksa} \end{aligned} \tag{16}$$

And the inverse transformation is given by the inverse Fourier transform

$$\begin{aligned} Q_k &= \frac{1}{\sqrt{N}} \sum_s q_s e^{-iksa} \\ Q_k &= \frac{1}{\sqrt{N}} \sum_s p_s e^{iksa} \end{aligned} \tag{17}$$

Expressing the Hamiltonian in this new basis leds to the following expression

$$H = \sum_k \left\{ \frac{1}{2m} P_k P_{-k} k_e Q_k Q_{-k} \left(1 - \cos ka\right) \right\} \tag{18}$$

Now we can define a frequency given by

$$w_k{}^2 \equiv \frac{2k_e}{m}(1-\cos ka) \tag{19}$$

so that the new Hamiltonian has the form of a sum of simple harmonic oscillators

$$H = \sum_k \left\{ \frac{1}{2m} P_k P_{-k} + \frac{1}{2}\omega_k{}^2 Q_k Q_{-k} \right\} \tag{20}$$

As the energy of each harmonic oscillator is given by Eq. (15), the total energy of the system will be given by

$$E = \sum_k \varepsilon_k = \sum_k \left(n_k + \frac{1}{2}\right)\hbar\omega_k \tag{21}$$

Then we can conclude that the energy of the system is quantized, that is to say that not all kind of waves are allowed or that the amplitudes of these waves are also quantized. Now with a more sophisticated quantum treatment we can obtain some important results about the nature of these waves, which will show that can be understood as particle-like bosons.

The Hamiltonian, which is an operator in quantum mechanics, can be expressed in terms of two operators given by a linear combination of the momentum and position variables. These operators are defined by the following expressions

$$\begin{aligned} a_k &= \sqrt{\frac{m\omega_k}{2\hbar}}\left(Q_k - i\frac{P_k}{m\omega_k}\right) \\ a_k^\dagger &= \sqrt{\frac{m\omega_k}{2\hbar}}\left(Q_k + i\frac{P_k}{m\omega_k}\right) \end{aligned} \tag{22}$$

With these definitions, the Hamiltonian transform into an even simpler one

$$H = \sum_k \hbar\omega_k \left(a^\dagger{}_k a_k + \frac{1}{2}\right) \tag{23}$$

It can be proved that when acting the operators defined in Eq. (22) into the eigenstates of the Hamiltonian one get the upper or lower eigenstate, which is the same to say that the operators in Eq. (22) increase or decrease the energy of the oscillator. Mathematically it is [1]

$$\begin{aligned} a^\dagger{}_k \left|n_1, n_2, ..., n_k, ...n_N\right\rangle &= \sqrt{n_k+1}\left|n_1, n_2, ..., n_k+1, ...n_N\right\rangle \\ a_k \left|n_1, n_2, ..., n_k, ...n_N\right\rangle &= \sqrt{n_k}\left|n_1, n_2, ..., n_k-1, ...n_N\right\rangle \end{aligned} \tag{24}$$

Moreover, as all operators in quantum mechanics, they follow a specific commutation rules

$$[a_k, a_{k'}] = \left[a^\dagger{}_k, a^{\dagger'}_k\right] = 0 \qquad \left[a_k, a^\dagger{}_k\right] = \delta_{kk'} \tag{25}$$

As might be clear, the energy of each state of the system is given by the eigenvalue of the corresponding eigenstate of the Hamiltonian. So we can find the energy of the different states as follows

$$H\left|n\right\rangle = E\left|n\right\rangle$$

For our Hamiltonian, using the relations in Eq. (24) we have

$$H\left|n_1, n_2, ..., n_k, ...n_N\right\rangle = \sum_k \hbar\omega_k \left(a_k a^\dagger{}_k + \frac{1}{2}\right)\left|n_1, n_2, ..., n_k, ...n_N\right\rangle =$$

[1] The eigenstate $\left|n_1, n_2, ..., n_k, ...n_N\right\rangle$ means thah the first oscillator is in the state n_1, the second in the state n_2 and so on

$$= \sum_k \hbar\omega_k \left(n_k + \frac{1}{2}\right) |n_1, n_2, ..., n_k, ...n_N\rangle \Longrightarrow E = \sum_k \hbar\omega_k \left(n_k + \frac{1}{2}\right)$$

So the energy of the system when it is in its state $|n_1, n_2, ..., n_k, ...n_N\rangle$ is given by

$$E = \sum_k \hbar\omega_k \left(n_k + \frac{1}{2}\right) \tag{26}$$

in agreement with Eq. (21).

So, with this formalism we see that applying ${a^\dagger}_k$ to an eigenstate of the Hamiltonian we raise a level the oscillator k. If we consider the ground state of the system it's clearly given by $|0, 0, 0..., 0\rangle$ and it has energy $\varepsilon_0 = \sum_k \hbar\omega_k/2$. If all the frequencies were the same, then the vacuum energy would be $\varepsilon_0 = N\hbar\omega/2$, and if we let N tend to infinity, which is consistent in the thermodynamic limit, we would end up with an infinite zero-state energy. This problem is solved in Quantum Field Theory applying what is called *normal ordering*, which basically considers that the important thing to take into account is the energy difference between the different states of the system. In this manner, defining a presumably consistent mathematical operation the infinity can be removed [5].

Then, another approach can be used. Now consider the ground state as $|0\rangle$, which can be understood as if the system had no particles. Then, when a $a_k^\dagger$ is applied to the ground state we can think that it creates a particle, and the new state of the system is given by $|1\rangle$ with energy $\frac{3}{2}\hbar\omega_k$. With the a operator we would have the opposite thing, we would destroy a particle. For this reason this operators are named creation and annihilation operators, respectively. By consecutively applying this operator we can create or destroy as particles as times as the operator is applied. The subindex k in $a_k^\dagger$ or a_k denotes that this operator will create or destroy a particle of energy $\hbar\omega_k/2$, so to be clearer with this approach we can use $a^\dagger(\omega_k)$ or $a(\omega_k)$. Finally we can find the nature of this quasi-particles, this is to say if they are bosons or fermions. Consider a system of two particles, that in this approach will be given by

$$|\omega_k, \omega_{k'}\rangle = a^\dagger(\omega_k)a^\dagger(\omega_{k'})\,|0\rangle$$

From the commutation relation in Eq. (25) we can see that

$$|\omega_{k'}, \omega_k\rangle = |\omega_k, \omega_{k'}\rangle \Longleftrightarrow a^\dagger(\omega_k)a^\dagger(\omega_{k'}) = a^\dagger(\omega_{k'})a^\dagger(\omega_k)$$

Thus our particles are bosons, as the state is symmetric, and they are called *phonons*.

In summary, we have shown the wave behaviour of phonons, when considering a classical system, as its particle-like behaviour when considering the quantum treatment. In the wave representation we give them properties such as frequency, wave vector, velocity and of course energy. Then in the quantum representation we show that these waves can be thought as particle-like bosons with the important property that an increase of energy $\hbar\omega_k/2$ of the wave, in classical theory, can be thought as the creation of a new phonon of frequency ω_k. This property will be very useful in our work, as will be noticed later.

2.3 Boltzman Transport Equation

As said in the introduction section Section 1 it has been observed that Fourier model fails when modelling heat conduction in length scales smaller than a micron. The two main reasons of this mismatch between the Fourier model and experimental results in this spatial scales are the following:

1. Fourier's diffusive equation (FDE), as it names indicates, assume several phonon-phonon interactions while phonons travel through the domain, that is to say the material size between the boundaries. By the way, at this length scales the mean free path (MFP) of the phonon is greater than the material size, so the assumption made by Fourier's model is not valid.

2. Moreover, FDE admits to infinite speed of heat transport, which is contradictory to reality [3].

Hence, FDE is inappropiate to describe heat transport in small time and spatial scales. Instead, Boltzmann Transport Equation (BTE) has been widely used to study and model collection of particles that interact with each other by short range forces and follow a certain statistical distribution. Assuming that the particle-like behaviour of phonons is more significant than its wave-like behaviour, which is valid when the spatial scale is larger than the wavelength of phonons, the BTE can be used to solve heat transfer.

The general form of BTE is given by [6] [3]

$$\frac{\partial f}{\partial t} + \boldsymbol{v}_g \boldsymbol{\nabla} f + \boldsymbol{a} \frac{\partial f}{\partial \boldsymbol{v}_g} = \left(\frac{\partial f}{\partial t}\right)_{scattering} \tag{27}$$

where f is the distribution function of the phonons, t is the time, $\boldsymbol{a}$ the acceleration under a external force and $\boldsymbol{v}_g$ the group velocity. Note that the distribution function is in fact a function of position, wave vector and time $f = f(\boldsymbol{r}, \boldsymbol{k}, t)$ [2] [6].

In absence of an external force, which is what we will have in the present study, the BTE reduces to the following expression

$$\frac{\partial f}{\partial t} + \boldsymbol{v}_g \boldsymbol{\nabla} f = \left(\frac{\partial f}{\partial t}\right)_{scattering} \tag{28}$$

It is intuitive to see that the LHS of Eq. (28) accounts for the change of distribution function due to the drifting proces, while the RHS is the rate of change of the distribution function with respect to time due to scattering with other phonons. In general, this rate of change expressed in the RHS of Eq. (28) is given by the master equation

$$\left(\frac{\partial f}{\partial t}\right)_{scattering} = \sum_{\boldsymbol{k'}} \{\Phi(\boldsymbol{k'}, \boldsymbol{k}) f(\boldsymbol{k'}) - \Phi(\boldsymbol{k}, \boldsymbol{k'}) f(\boldsymbol{k})\} \tag{29}$$

where $\Phi(\boldsymbol{k}, \boldsymbol{k'})$ is the probability per unit time that a phonon of wave vector $\boldsymbol{k}$ change to a phonon of wave vector $\boldsymbol{k'}$ (the same is applied to $\Phi(\boldsymbol{k'}, \boldsymbol{k})$ in the opposite direction).

As $f = f(\boldsymbol{r}, \boldsymbol{k}, t)$ is a function of several variables it is in general difficult to solve. To make it solvable some approximation techniques have been developed. One of the most widely used approximation is the so called relaxation time approximation, which basically linearizes the scattering term of the BTE and implies that whenever the system is not in equilibrium the scattering term will restore it following an exponential decay law [3] [7].

Mathematically, the relaxation time approximation reads as

$$\left(\frac{\partial f}{\partial t}\right)_{scattering} = \frac{n - f}{\tau} \tag{30}$$

where n is the distribution function of phonons in equilibrium, which is given by Bose-Einstein distribution function (BE), as phonons are bosons. The τ parameter can be physically understood as the typical scattering time, this is to say the time needed for a phonon to interact with anoher phonon.

By manipulating the equation and integrating it we find the exponential decay law above mentioned

$$\int \frac{\partial f}{n - f} = \int \frac{\partial t}{\tau} \Longrightarrow n - f = e^{-t/\tau} \Longrightarrow f = n - e^{-t/\tau} \tag{31}$$

Then from Eq. (31) it is clear that for large time, $t \gg \tau$, the distribution functions of phonons f will tend to the equilibrium distribution function n. Thus, we can say that the scattering term in BTE tends to restore the equilibrium in the system.

2.4 Ballistic and diffusive regimes

From the scattering part of the BTE two main approximations can be considered: the ballistic and the diffusive regimes.

For the **ballistic regime** one consider the scattering events negligible, this is to say that the scattering part of the BTE is set to 0. As this is a typical radiation heat transfer process, it is well described at equilibrium by the Stefan Boltzman law of the black body radiation. From this law the steady state temperature is given by

$$T_{\text{steady}} = \left(\frac{{T_h}^4 + T_c^4}{2} \right)^{1/4} \tag{32}$$

For the **diffusive regime** an infinite number of scattering events are considered, being diffusion the main process governing heat transport. Thus, we need to solve the Fourier's heat equation.[1]

$$\frac{\partial T}{\partial t} = D \frac{\partial^2 T}{\partial x^2} \tag{33}$$

In equilibrium, temperature does not change with time

$$\frac{\partial^2 T}{\partial x^2} = 0 \Longrightarrow \frac{\partial T}{\partial x} = \text{const} \Longrightarrow T = Ax + B \tag{34}$$

Now applying boundary conditions we just need to solve a system of equations to find the steady state temperature profile

$$\begin{cases} T_{x=x_0} = T_0 \quad \longrightarrow \quad T_0 = Ax_0 + B \\ T_{x=x_f} = T_f \quad \longrightarrow \quad T_f = Ax_f + B \end{cases} \Longrightarrow T_f - T_0 = A(x_f - x_0) \Longrightarrow A = \frac{T_f - T_0}{x_f - x_0}$$

Now substituting the first of the boundary equations we can get $B = T_0 - \dfrac{T_f - T_0}{x_f - x_0} \cdot x_0$. And finally substituting the constants in Eq. (34) we obtain the steady state temperature profile

$$T_{\text{steady}} = \frac{T_f - T_0}{x_f - x_0} (x - x_0) + T_0 \tag{35}$$

2.5 Conductivity and conductance

Thermal conductivity κ measures the performance of a material in heat conduction and gives information about the heat flux (or energy flux) transported through the material per unit temperature and unit length. Hence, thermal conductivity is defined by the following equation

$$\boldsymbol{q} = \kappa \boldsymbol{\nabla} T \Longrightarrow \kappa \tag{36}$$

If we consider a one dimensional homogeneous system, conductivity can be calculated as follows

$$\kappa = \frac{qL}{\Delta T} \tag{37}$$

If we are in the ballistic regime the heat flux value is independent of the length scale, and as the boundary temperatures are fixed we realise that conductivity is proportional to the length of the system, $\kappa \propto L$. On the other hand, if we consider the diffusive regime it can be shown that thermal conductivity stays constant while the size scale of the system changes, as it also change the heat flow.

Finally, thermal conductance is defined as the thermal conductivity per unit length, $K = \kappa / L$. Thus for the ballistic regime it will be constant while it have a $1/L$ dependence in the diffusive regime.

[1] The one dimensional case is considered for consistency with the results shown later.

3 Gray Model

The simplest phonon transport model to solve the phonon BTE is called the Gray Model or Gray Media approach. In this model, the phonon properties depend only on temperature, being independent of frequencies and polarizations [3] [8], so that phonon properties are computed as averages based on local cell temperatures. The Monte Carlo method is applied when considering the phonon-phonon scattering, as a probabilistic approach for the phonon-phonon interaction is adopted in this model. Employing a single relaxation time approximation, τ, based on the mean free path of the phonon, the scattering probability is computed. As the contribution of optical phonons towards the thermal conductivity in nanostructures is very less compared to acoustic phonons [8] [3] only the acoustical band will be considered in the model.

To perform the simulation some previous calculations need to be done. Some of them are simple parameters that can be calculated analytically making some assumptions and considerations while some others need to be computed numerically. These calculations are shown in the following subsections.

3.1 Basic parameters

As shown in Section 2.1 the magnitude of maximum wave vector k_{max} in the first Brillouin zone depends on the inter-atomic distance a. For acoustical phonons, which are the only considered in the model, the maximum value for the wave vector corresponds with the maximum frequency reached in the first Brillouin zone, as can be seen in Fig. 2. Some different considerations can be done to find this lattice parameter: for example [3] uses $a = (N * m/\rho)^{1/3}$ considering a cubic cell structure, where N is the number of atoms in a cell ρ the density of the cell and m the mass of a single atom. Using this expression and the appropriate experimental values one gets the following results

$$\begin{aligned} a_{Ge} &= 0.566\,\text{nm} \\ a_{Si} &= 0.543\,\text{nm} \end{aligned} \tag{38}$$

This leads to the following values for the maximum wave vector of each material

$$\begin{aligned} k_{max\,Ge} &= \frac{\pi}{a_{Ge}} = 5.55 \times 10^9\,\text{m}^{-1} \\ k_{max\,Si} &= \frac{\pi}{a_{Si}} = 5.79 \times 10^9\,\text{m}^{-1} \end{aligned} \tag{39}$$

3.2 Dispersion relation

Following the approach taken in [3] each phonon dispersion branch is treated within the isotropic Brillouin zone approximated by a quadratic curve fit given by

$$\omega_k = \omega_0 + vk + ck^2 \tag{40}$$

From experimental data this v and c parameters can be obtained. The parameters obtained in [3] are summarised in the following tables

Table 1: Curve fitting parameters for Germanium

Polarization	ω_0 (10^{13} rad/s)	v (10^3 m/s)	c (10^{-7} m^2/s)
LA	0.00	5.30	-1.2
TA	0.00	2.26	-0.82
LO	5.70	-0.99	-0.48
TO	5.5	-0.18	0.00

Now from Table 1 we can compute the maximum frequency of the phonons in the first Brillouin zone for each polarization, as it is given by the dispersion relation curve fit Eq. (40) when $k = k_{max}$.

Table 2: Maximum frequency values for germanium

Polarization	ω_{max} (rad/s)
LA	4.406×10^{13}
TA	1.498×10^{13}

3.3 Thermal properties

Until now we have basically been treating phonons as individual particles or waves. However, what we should think about in order to model reality is a ensemble of phonons in a thermal bath. As shown in section Section 2.2 the quantum formalism of phonons leads to consider that this quasiparticles can be created and destroyed and that they interact with each other behaving like bosons. For this reason, when treating with an ensemble of such particles the statistical formalism to consider is the grand canonical ensemble.

Thus, all the thermal properties of the phonon ensemble can be derived from this formalism.

3.3.1 Equilibrium distribution function

Because phonons are bosons, the equilibrium distribution function for an ensemble of them in a thermal bath will be given by the Bose-Einstein distribution function

$$\langle n \rangle = \frac{1}{\exp\left(\frac{\varepsilon - \mu}{k_B T}\right) - 1} \tag{41}$$

As number of phonons is not conserved, because they are continuously being created and destroyed, the quimical potential μ must vanish, as it won't be a thermodynamic quantity appearing in the state equations. Then, the B-E distribution function will depend only on the energy of the state considered which can be expressed in terms of the frequency by $\varepsilon = \hbar\omega$ as phonons are treated as harmonic oscillators. Finally, as the frequency of a given state depends on the wave vector and polarization it is a good practice to express the equilibrium distribution function of the system as follows

$$\langle n_{k,p} \rangle = \frac{1}{\exp\left(\frac{\hbar\omega}{k_B T}\right) - 1} \tag{42}$$

3.3.2 Energy degeneracy or density of states

Following the statistical mechanics formalism adopted we can derive the energy degeneracy from the volume of the phase space Γ. Equivalently we can use the frequency degeneracy as energy and frequency are related

$$D(\omega) = \frac{\partial}{\partial \omega} \Gamma(\omega) \tag{43}$$

The phase space volume is compted as follows

$$\Gamma = \frac{1}{h^3} \int \mathrm{d}^3 q \mathrm{d}^3 p = \frac{4\pi V}{h^3} \int p^2 \mathrm{d}p = \frac{4\pi V}{h^3} \hbar^3 \int k^2 \mathrm{d}k = \frac{V}{2\pi^2} \int k^2 \frac{\mathrm{d}k}{\mathrm{d}\omega} \mathrm{d}\omega \tag{44}$$

where a change of variables $p = \hbar k \implies \mathrm{d}p = \hbar \mathrm{d}k$ has been used.

Then from Eq. (43) is straightforward that the density of states is given by

$$D(\omega) = \frac{Vk^2}{2\pi^2}\frac{\mathrm{d}k}{\mathrm{d}\omega} = \frac{Vk^2}{2\pi^2 v_g} \tag{45}$$

Where v_g is the group velocity, which is defined by $v_g = \frac{\partial\omega}{\partial k}$. As the wave vector and group velocity depends on polarization $D_p(\omega)$ should be written.

3.3.3 Energy

The total energy of the ensemble can be calculated by summation of the energy of each state and computed for each polarization. From our derivation each state is characterised by a frequency. The number of states of frequency ω is given by the product of the equilibrium function and the density of states for this frequency.[1]

$$E = \sum_p \sum_k \left(\langle n_{k,p} \rangle + \frac{1}{2} \right) \hbar\omega \tag{46}$$

Assuming that the phonon wave vectors are sufficiently dense in the k space, the summation over k can be replaced by an integral. Moreover, using the density of states $D_p(\omega)$, we can achieve the integration in the frequency domain. [9]. As discussed in 2.1 there is a maximum value for the frequency for each polarization, so there is an upper limit in each integral

$$E = \sum_p \int_0^{\omega_{\mathrm{max,p}}} \left(\langle n_{\omega,p} \rangle + \frac{1}{2} \right) D_p(\omega) g_p \hbar\omega \mathrm{d}\omega \tag{47}$$

where g_p is the degeneracy of each polarization band, that is to say $g_p = 2$ for transverse polarization and $g_p = 1$ for longitudinal polarization.

The $\frac{1}{2}$ term in the above equation is the constant zero point energy which does not participate in the energy transfer of the material, therefore it can been suppressed. Finally the total energy of the system will be given by

$$E = \sum_p \int_0^{\omega_{\mathrm{max,p}}} \langle n_{\omega,p} \rangle \, D_p(\omega) g_p \hbar\omega \mathrm{d}\omega = \frac{V}{2\pi^2} \sum_p \int_0^{\omega_{\mathrm{max,p}}} \frac{1}{\exp\left(\frac{\hbar\omega}{k_B T}\right) - 1} \frac{k_p^2}{v_{g_p}} g_p \mathrm{d}\omega \tag{48}$$

3.3.4 Phonon number density

Number density function N computes the number of phonons contained in a volume V for a given temperature T. It is given by the integral of the number of phonons per state over all possible states.

$$N = \sum_p \int_0^{\omega_{\mathrm{max,p}}} \langle n_{\omega,p} \rangle \, D_p(\omega) g_p \mathrm{d}\omega = \frac{V}{2\pi^2} \sum_p \int_0^{\omega_{\mathrm{max,\ p}}} \frac{1}{\exp\left(\frac{\hbar\omega}{k_B T}\right) - 1} \frac{k_p^2}{v_{g_p}} g_p \mathrm{d}\omega \tag{49}$$

Then from Eq. (49) and Eq. (48) the energy per phonon can be simply calculated by dividing E/N.

3.3.5 Average frequency

In the gray model the frequency of phonons at the same temperature is assumed to be the same and equal to the average frequency calculated for that particular temperature [3] [8].

The total energy in Eq. (48) can also be defined as the product of the average frequency by the number of phonons with the corresponding $\hbar$ constant

$$E = N\hbar\omega_{\mathrm{avg}} \tag{50}$$

[1] It can be thought as the product of the occupation probability of a state of frequency ω and the number of states of this frequency

Then the average frequency can be calculated as follows

$$\omega_{\text{avg}} = \frac{1}{N}\sum_p \int_0^{\omega_{\text{max, p}}} \omega \left\langle n_{\omega,p} \right\rangle D_p(\omega) g_p \mathrm{d}\omega = \frac{V}{2\pi^2 N}\sum_p \int_0^{\omega_{\text{max, p}}} \frac{\omega}{\exp\left(\frac{\hbar\omega}{k_B T}\right) - 1} \frac{k_p^2}{v_{g_p}} g_p \mathrm{d}\omega \tag{51}$$

3.3.6 Average group velocity

As the group velocity is defined by $\frac{\partial \omega}{\partial k}$ the average group velocity will be given by the following expression

$$v_{\text{avg}} = \frac{1}{N}\sum_p \int_0^{\omega_{\text{max,p}}} \frac{\partial \omega}{\partial k} \left\langle n_{\omega,p} \right\rangle D_p(\omega) \mathrm{d}\omega = \frac{V}{2\pi^2 N}\sum_p \int_0^{\omega_{\text{max, p}}} \frac{1}{\exp\left(\frac{\hbar\omega}{k_B T}\right) - 1} k_p^2 g_p \mathrm{d}\omega \tag{52}$$

3.3.7 Heat capacity

Directly from thermodynamics, the heat capacity at constant volume is defined as the ratio of energy absorbed by a substance to the corresponding change in temperature. In its differential form it is written as

$$C_V = \frac{\mathrm{d}E}{\mathrm{d}T} \tag{53}$$

Then heat capacity can be computed from Eq. (48) as follows

$$C_V = \frac{\mathrm{d}E}{\mathrm{d}T} = \sum_p \int_0^{\omega_{\text{max,p}}} \frac{\partial}{\partial T} \left\langle n_{\omega,p} \right\rangle D_p(\omega) \hbar\omega \mathrm{d}\omega \tag{54}$$

Taking the derivative of the equilibrium distribution function with respect to the temperature we achieve the following expression

$$C_V = \frac{V}{2\pi^2}\sum_p \int_0^{\omega_{\text{max,p}}} \frac{(\hbar\omega)^2 \exp\left(\frac{\hbar\omega}{k_B T}\right)}{T^2 \left(\exp\left(\frac{\hbar\omega}{k_B T}\right) - 1\right)^2} \frac{k_p^2}{v_{g_p}} g_p \mathrm{d}\omega \tag{55}$$

3.3.8 Mean free path

The mean free path λ, understood as the average distance travelled by a phonon before going into a scattering event, can be calculated from the kinetic theory of gases. The thermal conductivity of a gas is given by

$$\kappa_{\text{bulk}} = \frac{C_V v_{\text{avg}} \lambda}{3V} \tag{56}$$

where K_{bulk} is the bulk thermal conductivity of the material.

The experimental bulk conductivity for Germanium is given by

$$\kappa_{\text{bulkGe}} = 58\,\mathrm{W/m \cdot K} \tag{57}$$

3.3.9 Mean scattering time

The mean scattering time is the mean time elapsed between two consecutive scattering events in a phonon. It is directly related to the relaxation time aproximation, as it is the τ appearing in Eq. (31). This relaxation time can be computed directly from the mean free path and the average velocity of the phonons as

$$\tau = \frac{\lambda}{v_{\text{avg}}} = \frac{3V K_{\text{bulk}}}{{v_{\text{avg}}}^2 C_V} \tag{58}$$

3.4 Thermal properties calculations

In order to calculate all this expressions numerical integration has been applied. The results of the method are shown in the following figures

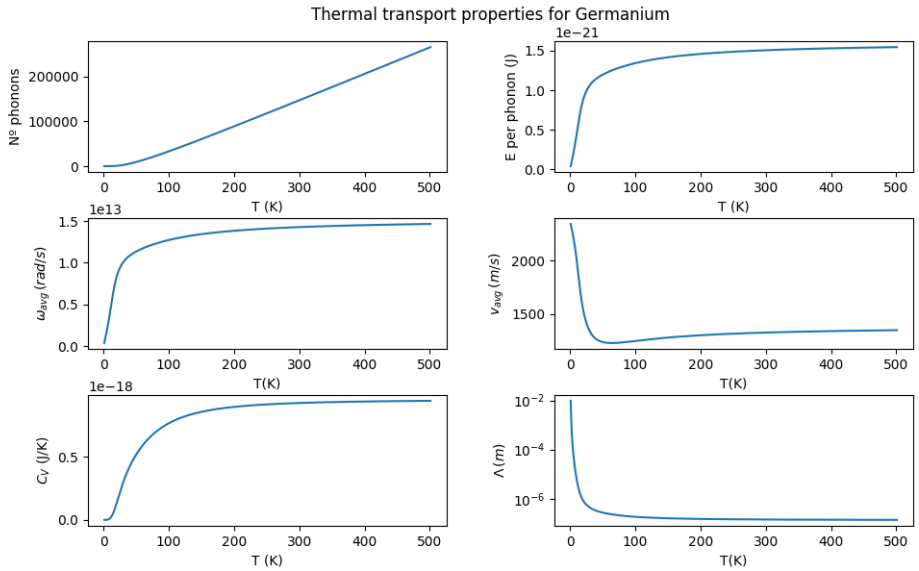

Figure 3: Thermal properties for Germanium

Fig. 3 shows the dependence of the phonon thermal properties on temperature, and the results are those expected. The existence of a maximum frequency value is confirmed and therefore a maximum energy per phonon value is observed. Finally, taking a look at the mean free path plot a logarithmic scale should be noted. It is important to set the logarithmic scale in the $y-axis$ as the mean free path of the phonon decreases rapidly with temperature, leading to a spatial multi-scale behaviour.

3.5 Simulation steps

Once all thermal properties of phonons are computed the simulation runs for a given number of time steps. In each of this time steps thermal properties are used to calculate sub-cell temperatures or consider phonon scattering events. In order to save computational time, the thermal properties of phonons are computed within a wide range of temperatures and then the information is stored in order to access to it later during the simulation. In this work each thermal property is stored in a *.npy* file as a *numpy ndarray*. This way, computational time is reduced as the integration to obtain the thermal properties is avoided at each time step.

The following flow chart shows schematically the simulation procedure

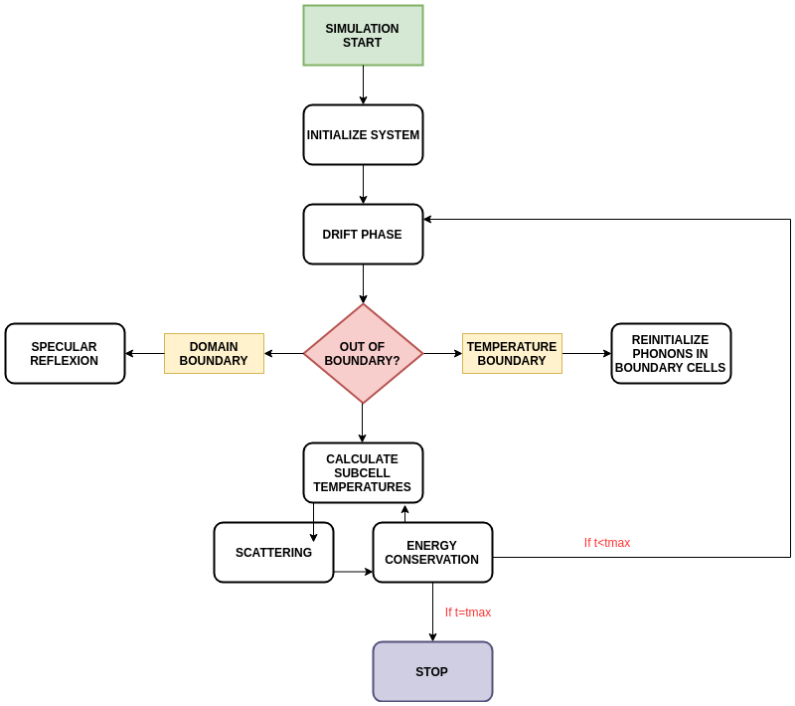

Figure 4: Simulation flow chart

3.5.1 General considerations

The domain of the simulation is divided in a certain number of sub-cells, initialised at a given temperature that will be evolving until it reaches a steady state. The time step can be chosen from different considerations

- The time step should be selected so that phonon can move at most the length of one sub-cell in one time step [3].
- In order to save computational effort the time step can be selected as one half of the smallest phonon scattering time given by Eq. (56) [10].

3.5.2 Initialise phonons

The first step in the simulation is to initialise each sub-cell with a number of predetermined phonons. The number of phonons to initialise depends directly on the initial temperature of the sub-cell and are given by equation Eq. (49).

After this calculation, which usually gives big numbers as can be seen in Fig. 3, a weighting factor W is employed to reduce computational time [10] [9], in spite of increasing the fluctuations of the system thermodynamic properties. Finally the initialised phonons are given by

$$N_{\text{init}} = \frac{N_{\text{calc}}}{W} \tag{59}$$

Then Eq. (59) indicates that one phonon in the simulation stands for W actual phonons.

Once the number of phonons in each sub-cell is determined we assign them the thermal properties computed in Section 3.3. This way each phonon has an energy, average velocity, average frequency, heat capacity and mean free path.

Finally we assign them a randomly chosen direction of movement in spherical coordinates. In this work this vector is multiplied by the average velocity for each phonon so we get the vector velocity of the phonons

3.5.3 Drift phase

The drift phase just performs a movement of the phonons by considering its given direction and average velocity. Then the new position of each phonon is calculated as

$$\boldsymbol{r}_{\text{new}} = \boldsymbol{r}_{\text{old}} + \boldsymbol{v} \cdot \mathrm{d}t \tag{60}$$

3.5.4 Boundary conditions

We use two kinds of boundary conditions in this work: specular reflective boundary condition, which can be understood as perfect smooth walls with adiabatic conditions and temperature boundaries, which define an isothermal condition.

- **Specular reflection** When phonons encounters this kind of boundaries they are specularly reflected back into the domain by changing the sign of the corresponding velocity vector components and correcting the trajectory. No other parameters are changed.
- **Temperature boundary** In this work temperature boundaries are implemented as temperature boundary cells which are at constant temperature during the whole simulation. At the end of every time step, all the phonons in temperature boundary cells are deleted. Then new phonons are initialised in these cells as in the initialisation step considering the cell temperatures.

3.5.5 Calculate sub-cell temperatures

To calculate sub-cell temperatures the total energy and number of phonons of each subcell is computed by summation. Then energy per phonon in each sub-cell can be obtained.

$$E = \sum_i W E_i \tag{61}$$

Therefore a match routine is established between the calculated value of the total energy in each sub-cell and the stored values of the total energy in function of temperature.

3.5.6 Scattering phase

In this specific step is where the Monte Carlo method is implemented, as in this work the phonon-phonon scattering takes a statistical approach. The relaxation time approximation mentioned in Section 2.3 is used to find the phonon scattering probability as follows.

From Eq. (31) the change in the distribution function of phonons due scattering in time is given by

$$\frac{\mathrm{d}f}{\mathrm{d}t} = \frac{e^{-t/\tau}}{\tau} \tag{62}$$

as clearly $\frac{\mathrm{d}n}{\mathrm{d}t} = 0$.

Then, as the change in the distribution function is checked for every time step in the simulation, the scattering probability is computed based on the $\mathrm{d}f$ term in the numerator of Eq. (62) [3]

$$\mathrm{d}f = e^{-t/\tau} = \exp\left(-\frac{t \cdot v_{\text{avg}}}{\lambda}\right) \tag{63}$$

Thus the scattering probability is given by

$$P_s = 1 - \exp\left(-\frac{t \cdot v_{\text{avg}}}{\lambda}\right) \tag{64}$$

where t is the elapsed time after the phonon last underwent the scattering process.

In order to implement the Monte Carlo method a few simple steps are followed for each phonon each time step in the simulation

1. Calculate phonon scattering probability P_s
2. Throw a uniform random dice whose values belong to the interval $[0, 1]$. We call the value obtained after throwing the dice P_d
3. Only if $P_s > P_d$ the phonon is scattered.
4. If the phonon is scattered its thermal properties as energy, heat capacity, average velocity, average frequency and mean free path are reset considering sub-cell temperature. The phonon direction vector is also randomly computed and assigned.

As we can see from Eq. (64) when the time elapsed since the last scattering event is 0 the scattering probability is also 0, while when this elapsed time is long the probability tends to 1. This make sense with the relaxation time approximation and presumably with reality.

3.5.7 Energy conservation

When phonon's physical parameters are changed in the phonon-phonon scattering process the energy might not be conserved. For this reason we must impose energy conservation in our code, so that energy is conserved in each sub-cell within a tolerance value. This tolerance value is given by the maximum energy of a phonon $E_{\max}\hbar\omega_{\max}$.
The following scheme is used to implement this energy conservation:

1. Calculate the energy of each sub-cell before the scattering process and store it as the initial energy.
2. Calculate the energy of each sub-cell after the scattering process and store it as the final energy
3. Compute the energy difference of each subcell $\Delta E_i = E_{f_i} - E_{0i}$
   - If $\Delta E_i > E_{\max}$ there is a gain of energy so we must delete the number of phonons that correspond to this amount of energy. To do it, an iterative method is implemented, deleting a phonon in each iteration and recalculating energy difference. The method finishes when the energy difference is below the tolerance.
   - If $-\Delta E_i > E_{\max}$ there is a loss of energy so we must create the number of phonons that correspond to this amount of energy. The created phonons are assigned thermal properties based on local sub-cell temperature. To do it, an iterative method is implemented, creating a phonon in each iteration and recalculating energy difference. The method finishes when the energy difference is below the tolerance.

3.5.8 Finishing the time step

Finally temperature is again computed in all the sub-cells and all the method from the drift step is repeated the number of times desired.

3.6 Software documentation

The software created for this work has been upload in a GitHub repository. There, a little documentation has been written along with some useful examples, which reproduce a part of the results presented in the following section.

The repository can be visited in https://github.com/agimenezromero/NHT-Gray-Model

4 Results and discussion

First of all, in order to verify the computational model implemented, some analytically solvable systems are simulated. As this work approach includes ballistic and diffusive regimes of heat transport both will be verified. Then the effect on heat transport given by the size of the system or the roughness of the wall's surface will be studied. Finally conductivity and conductance for different systems are computed and compared with experimental data.

4.1 Ballistic transport in 1D bulk Germanium

When the mean free path of the phonons is much greater than the domain length, phonons will interact with the isothermal boundaries before than with each other. Thus, the most part of the phonons will be annihilated before going under scattering, which leads to ballistic heat transport. As this is a typical radiation heat transfer process, it is well described at equilibrium by the Stefan Boltzman law of the black body radiation. From this law the steady state temperature is given by

$$T_{\text{steady}} = \left(\frac{{T_h}^4 + T_c^4}{2} \right)^{1/4} \tag{65}$$

where T_h and T_c are the boundary hot and cold temperatures at the end cells.

For length scales of some nanometers, to reach the ballistic regime the temperature must be about few kelvin. The reason is that for higher temperatures the MFP of the phonons is of the order of 100 nm or less, which is not much longer than the domain size. To simulate such a case in bulk germanium the following parameters are used

Table 3: Parameters used for the ballistic case validation

Domain $(x \times y \times z)$ [nm]	Sub-cells $(x \times y \times z)$ [nm]	T_h [K]	T_c [K]	T_i [K]	Δt [ps]	t_{MAX} [ns]	W
$(10 \times 10 \times 10)$	$(0.5 \times 10 \times 10)$	11.88	3	5	0.1	10	0.05

The hotter phonons, this is to say the phonons emitted at $T = 11.88\,\text{K}$, will have the smaller mean free path for the current simulation. The MFP value for phonons at this temperature is $\lambda = 3.57\,\mu\text{m}$, which is 357 times larger than the domain length of 10 nm. Thus, ballistic behaviour is expected to be shown by a constant steady state temperature given by Eq. (65) of $T_{steady} = 10\,\text{K}$.

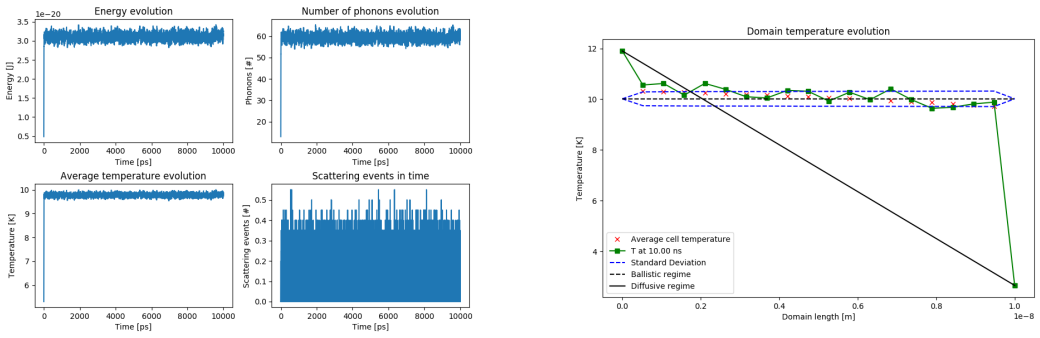

(a) Thermodynamic system properties

(b) Sub-cell temperature evolution

Figure 5: System temporal evolution for the ballistic case

Fig. 5(a) shows the time evolution of the thermodynamic quantities of the system: total energy, number of phonons, average total temperature and the number of scattering events. In Fig. 5(b) the sub-cell final and average temperature is represented, along with the standard deviation of the

average. It can be seen that temperature fluctuates between the standard deviation zone and that the average steady temperature fit with the predicted by the Stefan Boltzmann law. Moreover, the maximum deviation from the theoretical temperature is from 0.3 K, so the maximum error committed is about a 3%.

It can be noticed that there are significantly few scattering events every time step, accordingly with the ballistic regime main hypothesis. More precisely, the average number of phonons in equilibrium is about $N_{\text{eq}} \simeq 60$ while the average number of scattering events is $SE \simeq 0.1$. Then the fraction of the phonons going under scattering every time step is 1/600 or 0.17% which is a really low number.

The reason why the scattering events are not integers is the weighting factor employed, which is smaller than one. Thus, a phonon in the simulation stands for a fraction of a real phonon. This apparently contradictory use of the weighting factor is done to increase the number of phonons and improve the statistical sampling in this particular case, where there are just a few phonons because of the very low temperature considered (about 2 phonons per cell).

4.2 Diffusive transport in 1D bulk Germanium

At higher temperatures the MFP of the phonons is about $\lambda \sim 10^7$ m, so only materials with sizes much smaller than this length scale will reach ballistic behaviour. For larger devices the dominant regime will be diffusive, as many scattering events will occur before phonons get annihilated at the boundaries, so the steady state will be given by the Fourier law. In a one dimensional space, the Fouirer's law can be analytically solved (Section 2.4) and the resultant steady state temperature is given by

$$T_{\text{steady}} = \frac{T_f - T_0}{x_f - x_0} \cdot (x - x_0) + T_0 \tag{66}$$

To validate the diffusive regime the system reported in Table 4 has been simulated

Table 4: Parameters used for the diffusive case validation

Domain ($x \times y \times z$) [nm]	Sub-cells ($x \times y \times z$) [nm]	T_h [K]	T_c [K]	T_i [K]	Δt [ps]	t_{MAX} [ns]	W
$(500 \times 10 \times 10)$	$(10 \times 10 \times 10)$	150	100	125	5	50	5000

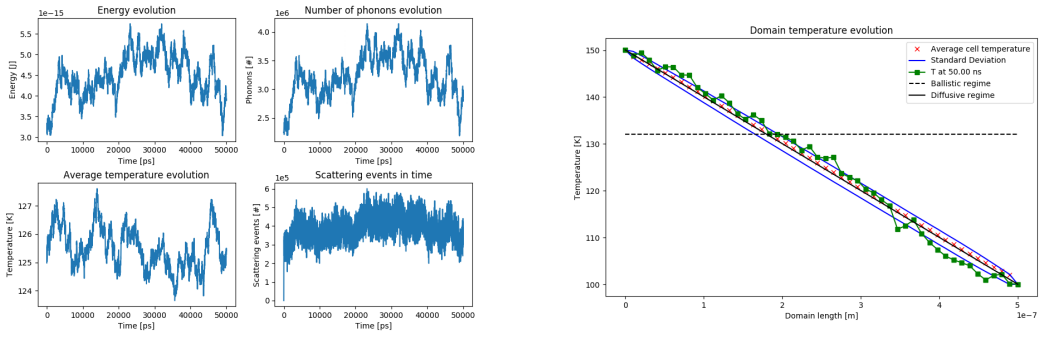

(a) Thermodynamic system properties

(b) Sub-cell temperature evolution

Figure 6: System temporal evolution for the diffusive case

Fig. 6(a) shows the evolution of the thermodynamic properties of the system and ensures that the steady state has been reached. The huge fluctuations observed are given by the big weighting factor used. On the other hand, Fig. 6(b) represent the temperature profile after 50 nanoseconds and the

average temperature of each of the sub-cells. It can be noticed that temperature fluctuations might exceed the standard deviation zone, which can be associated again with the use of a big weighting factor. Anyway, average cell temperature fits almost perfectly with the analytically predicted linear profile. Moreover, the maximum deviation of the average cell temperature from the expected profile temperature is of 1.6 K, which in the present temperature gradient is negligible.

In Fig. 6(a) the scattering events plot shows that many of the phonons go under scattering every time step. More precisely, the average number of scattering events is about $SE \simeq 3.8 \times 10^5$ while the average number of phonons in equilibrium is $N_{\text{eq}} \simeq 3.2 \times 10^6$. Thus the fraction of phonons interacting by scattering each time step is 39/320 or 12.19%. This number may not seem sufficiently large, but compared with the ballistic case it represents about 73 times more scattering events.

4.3 Size effect

As it have might be noticed, ballistic and diffusive regimes depend on temperature as well as on the length scale of the system. The reason is that the condition for the existence of one or the other regime is the comparison between the MFP of the phonons, given by boundary temperatures, and the length of the system. To show the size effect in the behaviour of heat transport, the high temperature diffusive system simulated above has been modified to achieve the opposite regime. For this purpose the domain length has been reduced into different values until reaching the ballistic regime.

All the parmeters used in the simulations can be found in Appendix A.

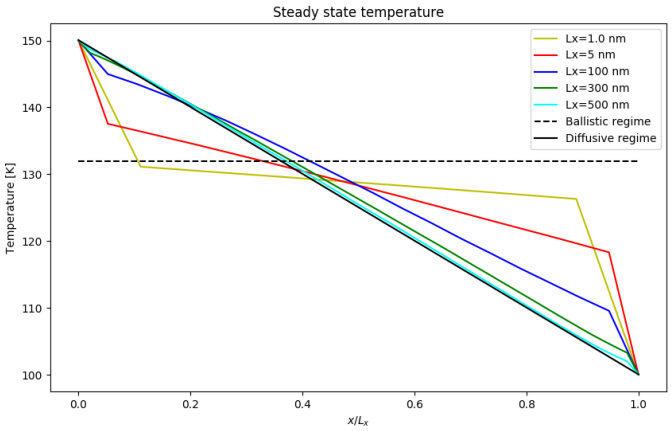

Figure 7: Size effect on heat transport

Fig. 7 shows the different steady states[1] reached by the systems modelled in Table 4 for different values of the domain length in the x direction. In order to plot all the different simulations with different length values in the same figure, it has been scaled to x/L_x in the x axis. As it was expected, the larger the system is the more diffusive the heat transport behave.

A part from checking that the transport regime does not depend only in temperature or the system length scale, rather than both at the same time, this size effect study validates the software developed to study intermediate regimes. Hence, some not analytical systems could be studied with it and comparing the outputs with experimental results the last validation of this work could be done.

[1] The ploted temperature line represents the average temperature for each cell sub-cell calculated as an ensemble average from the corresponding equilibrium time value.

4.4 Walls roughness effect

In Section 3.5 it is explained that the Gray Model approach considers specular reflection with the domain walls. Physically, this means that the walls are perfectly smooth, like mirrors, which can be far from reality for some particular systems. The roughness effect of the walls can be studied by considering diffusive scattering with the domain walls. In fact, some studies of this type have been made by considering a probabilistic approach, where not always the phonons reflect diffusively with the walls but it depends on a surface roughness parameter [11]. However, in this work a deterministic approach is considered by which all phonons colliding with the domain walls experiment a diffusive reflection, which means that the walls are very rough. Thus, for each reflection, all the phonon properties are changed by new ones based on average sub-cell temperature.

Then, even if the system is thought to be ballistic because of the temperature and spatial length conditions, a diffusive temperature profile is expected to be observed in the steady state. However, the width and height of the system now take an important role. To achieve a diffusive behaviour with ballistic temperature and length conditions, all the phonons should collide with the walls several times before annihilating in the isothermal boundaries. Then, it will be accomplished when $L_x \gg L_y, L_z$.

To validate the hypothesis made above the system described in Table 3 has been simulated again but introducing diffusive domain walls.

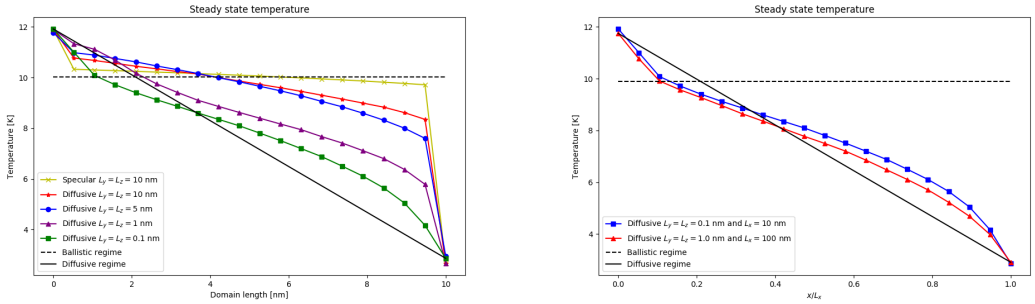

(a) $L_y = L_z$ variation with L_x fixed

(b) Same L_x/L_y with different values

Figure 8: Steady state temperature for different $L_y = L_z$ values

Fig. 8(a) shows the average steady state temperature reached by the different systems considered, which only differ on $L_y = L_z$ values, this is to say their width and height. It is clear that these values play an important role in the effect of the diffusive walls, but we must keep in mind that what really determine the effect of the diffusive walls is the comparison between the length of the system and its width and height. To intensify this hypothesis, Fig. 8(b) shows the effect of the diffusive walls for the same proportion between the length and the width (or height) of the system. It can bee seen that for the same proportion we get approximately the same result.

Then, from both figures the conclusion is clear. What determines the effect of the diffusive walls is the comparison between the length L_x of the system and its width, L_y and height, L_z. Thus, when the limit $L_x \gg L_y, L_z$ is accomplished the steady state temperature will be totally diffusive. All the parameters used in this simulations can be found in Appendix B.

4.5 Conductivity and conductance

Finally, thermal conductivity and conductance have been computed from the simulation heat flux outputs. To calculate heat flux, the software computes the number of phonons going through the middle plain of the simulation domain in each direction along with its energy every time step. This way the heat flux is obtained from the following equation

$$q = \frac{\Delta E}{A \cdot \mathrm{d}t} \tag{67}$$

Then thermal conductivity κ and thermal conductance K can be obtained directly from

$$\kappa = \frac{q}{T_h - T_c} \qquad K = \frac{\kappa}{L} \tag{68}$$

where T_h and T_c are the hot and cold boundary temperatures and L the system length.

In the figure below thermal conductivity and thermal conductance are shown for different simulated systems. All the simulations have been done within the same temperature boundaries and different lengths have been considered. All the parameters used in the simulations are reported in Appendix C.

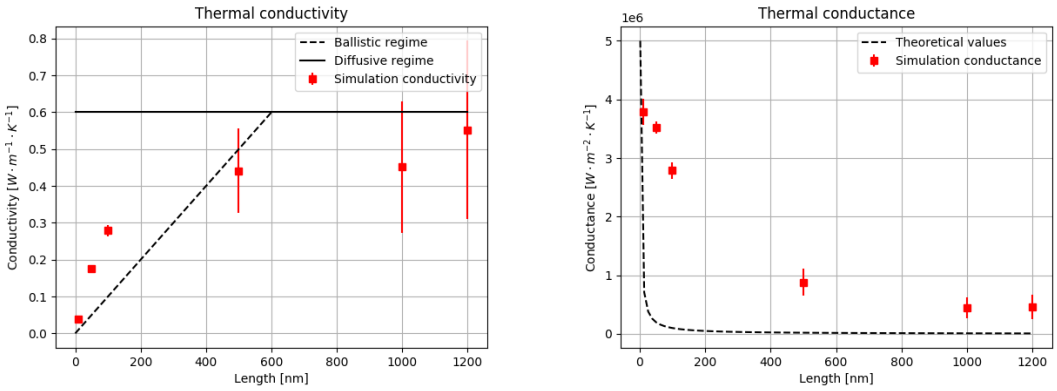

(a) Thermal conductivity vs system length

(b) Thermal conductance vs system length

Figure 9: Thermal conductivity and conductance from simulation

Fig. 9 show that the results retrived by the simulation follow approximately the form of the theoretical predictions. Nevertheless the values obtained are far from reality, as the thermal conductivity of bulk germanium within this temperatures should tend to values within $\kappa = 100\,\mathrm{W} \cdot \mathrm{m}^{-1}\mathrm{K}^{-1}$ and $\kappa = 1000\,\mathrm{W} \cdot \mathrm{m}^{-1}\mathrm{K}^{-1}$ [12].

This mismatch between the experimental conductivity values and the obtained with this work can be attributed to the huge number of approximations and simplifications done in the model. Although it has not been explained here, there are more sophisticated approaches to study thermal conductivity at nanoscale. For example, the so called Non Gray Model approach, which uses more exact considerations as frequency dependent phonon properties or three phonon scatterings, gives better results when computing thermal conductivity.

4.6 2D system

To finish with, a two dimensional system has been studied with the software developed. The aim of this particular case is nothing but study a non analytical case in a higher dimension, taking advantage of the fact that the software has been programmed even for a 3D general case. The system considered is formed by several sub-cells and diffusive walls. Table 5 details all the parameters used for this simulation.

Table 5: Parameters used for the 2D system simulation

Domain $(x \times y \times z)$ [nm]	Sub-cells $(x \times y \times z)$ [nm]	T_h [K]	T_c [K]	T_i [K]	Δt [ps]	t_{MAX} [ns]	W
$(100 \times 100 \times 10)$	$(10 \times 10 \times 10)$	11.88	3	5	0.05	10	1

For this temperatures the average MFP of the phonons is $5 \times 10^{-5}\,\mathrm{m} = 5 \times 10^{4}\,\mathrm{nm}$. As the system size is much shorter ballistic behaviour might be expected. However, the diffusive boundary walls must be taken into account. Here the diffusive walls in the z axis will play an important role, as $L_z \ll L_x$. Therefore a diffusive temperature profile will be imposed. Moreover, as it is a two dimensional system, now phonons can travel diagonally in the domain, so the diffusive hypothesis gets reinforced.

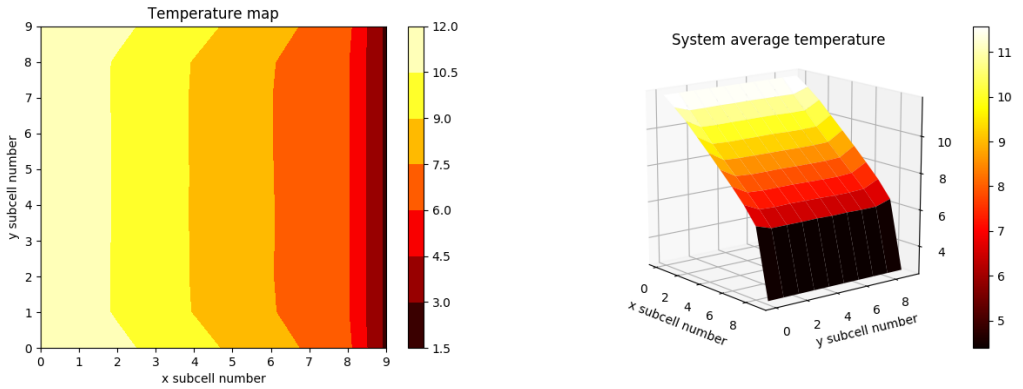

(a) Average temperature map (b) 3D representation

Figure 10: Average temperature of the system

Fig. 10 shows the average temperature of all the sub-cells. The same diffusive temperature profile is observed in all the cells except of those next to the walls. This little discrepancy can be attributed to the non-periodic boundary conditions existing in the walls. To account for the level of diffuseness of the system the temperature profiles for some planes can be represented in another figure.

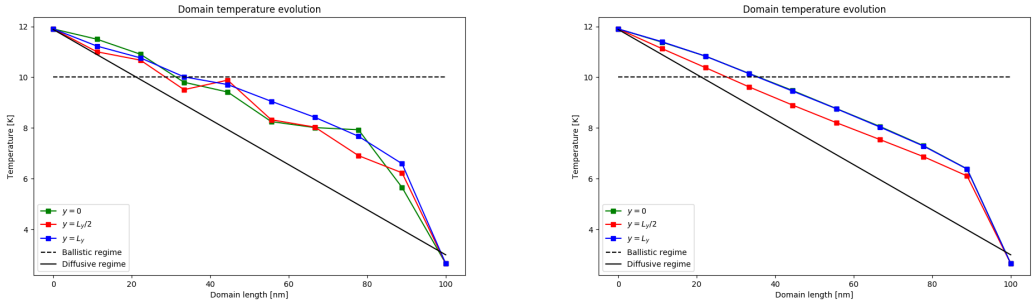

(a) Final linear temperature profile in some y planes (b) Average linear temperature profile in some y planes

Figure 11: Caption

Fig. 11(a) shows the last frame temperature profile in the x direction in different y planes while Fig. 11(b) represents its average. It can be seen how the average the cells near of each walls coincide, being a little bit less diffusive. As said before, this difference in the diffuseness might be caused by size effect, this is to say not periodic boundary conditions.

5 Conclusions

In this work the thermal transport has been studied at nanometric scale from computer simulations. The approach considered is known as the Gray Model and consists in perform probabilistic phonon-phonon scattering events with an implemented Monte Carlo method. As seen in Section 4.1 and Section 4.2 the model has been tested with analytically solvable systems and its performance is in good agreement with theoretical results.

Then, other non analytical systems have been simulated and studied in Section 4.3 and Section 4.4. The results are in good agreement with the previous hypothesis made, which have a strong theoretical background support.

As a further step, conductivity and conductance have been computed from different simulations and its dependence with the length scale of the system has been studied. The results retrieved show the same dependence with the system length of that predicted by the theory. Nevertheless the fit is far from being exact and the values are even further to coincide with experimental results. As commented previously, this mismatch between experimental data and simulation results are associated with the simplified model considered and all its approximations.

Finally, a 2D system has been simulated successfully, even though more studies should be done to be sure of the reliability of the results (to prove the non periodic boundary conditions, for example).

6 Ongoing work

- Make specific experiments to compare with the simulations results of the software.
- Demonstrate the non periodic boundary conditions effect shown in Fig. 10. This can be done by performing simulations including periodic boundary conditions and state whether the effect disappears or not.
- Use this software to study 3D cases.
- Try to find a method to parallelize the code.
- Rewrite the library in C++ or similar non interpreted languages to improve computational time.

A Parameters used in the size effect study

Table 6: High temperature

Domain ($x \times y \times z$) [nm]	Sub-cells ($x \times y \times z$) [nm]	T_h [K]	T_c [K]	T_i [K]	Δt [ps]	t_{MAX} [ns]	W
$(1 \times 10 \times 10)$	$(0.1 \times 10 \times 10)$	150	100	125	0.05	2	2
$(5 \times 10 \times 10)$	$(0.25 \times 10 \times 10)$	150	100	125	0.1	2	10
$(100 \times 10 \times 10)$	$(5 \times 10 \times 10)$	150	100	125	4	5	300
$(300 \times 10 \times 10)$	$(6 \times 10 \times 10)$	150	100	125	4	20	1000
$(500 \times 10 \times 10)$	$(10 \times 10 \times 10)$	150	100	125	4	50	5000

B Parameters used in the roughness study

Table 7: Parameters used for the roughness study

Domain ($x \times y \times z$) [nm]	Sub-cells ($x \times y \times z$) [nm]	T_h [K]	T_c [K]	T_i [K]	Δt [ps]	t_{MAX} [ns]	W
$(10 \times 10 \times 10)$	$(0.5 \times 10 \times 10)$	11.88	3	5	0.1	1	0.05
$(10 \times 5 \times 5)$	$(0.5 \times 5 \times 5)$	11.88	3	5	0.1	1	0.01
$(10 \times 1 \times 1)$	$(0.5 \times 1 \times 1)$	11.88	3	5	0.05	1	10^{-3}
$(10 \times 0.5 \times 0.5)$	$(0.5 \times 1 \times 1)$	11.88	3	5	0.01	1	5×10^{-5}

C Parameters used in the conductivity and conductance study

Table 8: Low temperature

Domain ($x \times y \times z$) [nm]	Sub-cells ($x \times y \times z$) [nm]	T_h [K]	T_c [K]	T_i [K]	Δt [ps]	t_{MAX} [ns]	W
$(10 \times 10 \times 10)$	$(0.5 \times 10 \times 10)$	11.88	3	5	0.1	10	0.05
$(50 \times 10 \times 10)$	$(2.5 \times 10 \times 10)$	11.88	3	5	1	10	0.1
$(100 \times 10 \times 10)$	$(5 \times 10 \times 10)$	11.88	3	5	1	10	0.2
$(500 \times 10 \times 10)$	$(10 \times 10 \times 10)$	11.88	3	5	1	20	1
$(1000 \times 10 \times 10)$	$(20 \times 10 \times 10)$	11.88	3	5	1	20	1
$(1200 \times 10 \times 10)$	$(24 \times 10 \times 10)$	11.88	3	5	1	20	1

References

[1] Jean Baptiste Joseph Fourier. *Théorie Analytique de la Chaleur*. Cambridge Library Collection - Mathematics. Cambridge University Press, 2009. DOI: 10.1017/CBO9780511693229.

[2] Giuseppe Romano, Jean-Philippe Peraud, and Jeffrey Grossman. "Simulating Nanoscale Heat Transport". In: (June 2015). DOI: 10.1007/978-94-007-6178-0_100935-1.

[3] Mayank Malladi. *Phonon Transport Analysis of Semiconductor Nanocomposites using Monte Carlo Simulations*. 2013.

[4] Charles Kittel. *Introducción a la física del estado sòlido*. Editorial Reverté, 1998. ISBN: 84-291-4317-3.

[5] Eduard Massó. *Notes on Quantum Field Theory*. 2017.

[6] Jayathi Y. Murthy et al. "Review of Multiscale Simulation in Submicron Heat Transfer". In: *International Journal for Multiscale Computational Engineering - INT J MULTISCALE COMPUT ENG* 3 (Jan. 2005), pp. 5–32. DOI: 10.1615/IntJMultCompEng.v3.i1.20.

[7] Graz University of Technology. *Relaxation time approximation*. 2019. URL: http://lampx.tugraz.at/~hadley/ss2/transport/relax.php.

[8] Ming-Shan Jeng et al. "Modeling the Thermal Conductivity and Phonon Transport in Nanoparticle Composites Using Monte Carlo Simulation". In: *Journal of Heat Transfer-transactions of The Asme - J HEAT TRANSFER* 130 (Apr. 2008). DOI: 10.1115/1.2818765.

[9] David Lacroix, Karl Joulain, and Denis Lemonnier. "Monte Carlo transient phonon transport in silicon and germanium at nanoscales". In: *Phys. Rev. B* 72 (6 Aug. 2005), p. 064305. DOI: 10.1103/PhysRevB.72.064305. URL: https://link.aps.org/doi/10.1103/PhysRevB.72.064305.

[10] "Monte Carlo Simulation of Silicon Nanowire Thermal Conductivity". In: *Journal of Heat Transfer-transactions of The Asme - J HEAT TRANSFER* (May 2005), p. 9. DOI: 10.1115/1.2035114.

[11] Chandan Bera. "Monte Carlo simulation of thermal conductivity of Si nanowire: An investigation on the phonon confinement effect on the thermal transport". In: (Oct. 2012). DOI: 074323.

[12] G. K. White and S. B. Woods. "Thermal Conductivity of Germanium and Silicon at Low Temperatures". In: *Phys. Rev.* 103 (3 Aug. 1956), pp. 569–571. DOI: 10.1103/PhysRev.103.569. URL: https://link.aps.org/doi/10.1103/PhysRev.103.569.

[13] Jeremie Maire. "Thermal phonon transport in silicon nanostructures". Theses. Ecole Centrale de Lyon, Dec. 2015. URL: https://tel.archives-ouvertes.fr/tel-01374868.

[14] Basil T. Wong, Mathieu Francoeur, and M. Pinar Mengüç. "A Monte Carlo simulation for phonon transport within silicon structures at nanoscales with heat generation". In: *International Journal of Heat and Mass Transfer* 54.9 (2011), pp. 1825–1838. ISSN: 0017-9310. DOI: https://doi.org/10.1016/j.ijheatmasstransfer.2010.10.039. URL: http://www.sciencedirect.com/science/article/pii/S0017931011000329.